Sonochemical Synthesis and Characterization of Iron Oxide Coated on Submicrospherical Alumina: A Direct Observation of Interaction between Iron Oxide and Alumina

Z. Y. Zhong,[†] T. Prozorov,[‡] I. Felner,[§] and A. Gedanken*[,†]

Department of Chemistry, Bar-Ilan University, Ramat-Gan 52900, Israel, Department of Physics, Bar-Ilan University, Ramat-Gan 52900, Israel, and Racah Institute of Physics, Hebrew University, Jerusalem, Israel

Received: July 24, 1998; In Final Form: October 20, 1998

Coating of iron oxides on submicrospheres of alumina was carried out by the sonochemical method. Three kinds of alumina were used, namely, the as-prepared, 700 and 1000 °C heated-alumina. TEM results reveal various coating effects on different heat-treated substrates. The optimum coating is obtained on as-prepared amorphous alumina, in which most of the iron oxide particles are adhered to alumina spheres tightly, while in the sample coated on crystallized alumina heated at 1000 °C, most of the iron oxide particles remain separate from the alumina spheres. The strong interaction between iron oxides and alumina substrate was directly observed by XRD, TEM, and IR and magnetic measurements. Owing to the strong interaction between adhered iron particles and alumina substrate, the complete transformation of γ-Fe_2O_3 to α-Fe_2O_3 was retarded to higher than 700 °C; conversely, the presence of haematite can induce the formation of α-Al_2O_3 at the high temperatures. TEM images clearly show the changes of particle size and morphology for samples at the different heating stages and the combination degree of iron oxide with alumina substrate. At a low temperature, IR results show that iron or iron carbonyl compound is interacted with the isolated OH groups on alumina surface. At high temperatures, the iron ions can incorporate into the defect sites of alumina and form a solid solution at the interface. Magnetization measurements show the existence of elemental iron in as-prepared sample coated on crystallized alumina.

I. Introduction

Coated composite materials have attracted attention in recent years because of their potential application in industry and their importance in fundamental study. In particular, the development of effective coating techniques for metal and metal oxide on substrate and the interaction between coated metal elements with substrate have been of great interest to materials scientists[1,2] and catalysis chemists.[3,4]

It is known that the properties of coated composite materials are mainly determined by the coating materials and their structure. Conventional methods such as evaporation, impregnation, precipitation, and sputtering usually yield a coated polycrystalline product. In recent years, there have been many reports that nanostructured materials often exhibit unusual electrical, chemical, structural, and magnetic properties due to their unique structural characteristics, such as long-range disorder structure, the existence of a higher energy boundary, interface or surface region, etc. As reported by Susclick et al.,[5] sonochemistry can be used as a tool for the preparation of nanosized metals having an amorphous structure. The formation of the amorphous metals is due to the extreme conditions, such as the highest transient temperature, which exceeds 5000 K in localized hot spots, and the ultrafast cooling rate of $>10^{10}$ K s^{-1}, that can be obtained in sonication. Recently, sonication has been further developed as a tool to drive the deposition of iron oxide, metal nickel, and cobalt onto the surface of silica particles.[6,7,8] However, to materials scientists, because silica can form impurity phases with many coated magnetic materials,[9−11] which influences its magnetic properties, Al_2O_3 is a superior substrate as a matrix material. On the other hand, aluminas of various forms are the most commonly used materials as catalysts and their supports. Many attempts have been made over the past 40 years to understand the surface structure of various aluminas and the interaction between deposited elements and the alumina support.[12] However, there are still many questions under discussion. For example, the identification of different hydroxyl groups on the surface of alumina and their activity toward deposited metal elements are far from being agreed upon in the literature.[3,13] Thus, in this work, we aim to develop a general and efficient coating technique for Al_2O_3; furthermore, we want to study the interaction between coated metal and alumina, which has been believed to be the key factor in the understanding of the nature of catalysis, and to improve the property of composition materials as catalysts, in addition to other applications.

II. Experimental Section

Amorphous submicrospherical alumina was prepared by hydrolysis of aluminum *sec*-butoxide (ASB) in a dilute mixture solution of 1-octanol, 1-butanol, and acetonitrile, and in the preparation, hydroxypropylcellulose(HPC) was used as a dispersant.[14] First, the aluminum alkoxide was dissolved in 1-octanol at 60 °C. Then the defined amount of HPC (0.1×10^{-3} g/cm^{-3}) and acetonitrile were mixed. Meanwhile, water was dissolved in another mixture solution of 1-octanol and 1-butanol. The two solutions were mixed up with a magnetic stirrer at 25 °C for 30 s and aged for 30 min. The total initial mixed solution had a composition of approximately 1-octanol

* To whom correspondence should be addressed. Email: gedanken@mail.biu.ac.il.
[†] Department of Chemistry.
[‡] Department of Physics.

10.1021/jp983164z CCC: $18.00
Published on Web 02/11/1999

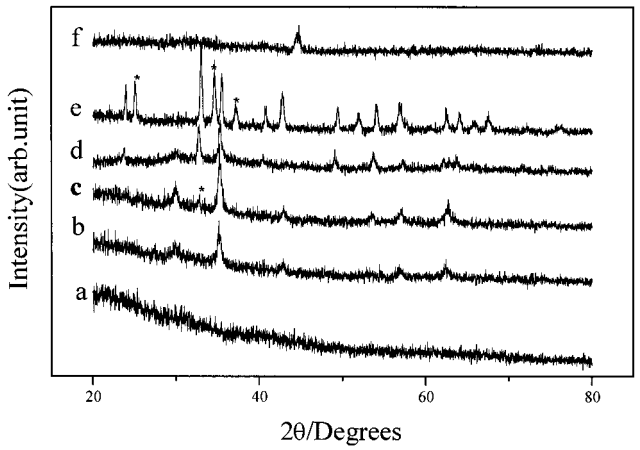

Figure 1. 1. XRD patterns of (line a) as-prepared sample of iron oxide coated on A-alumina, (line b) iron oxide coated on A-alumina and heated to 400 °C under argon, (line c) iron oxide coated on A-alumina and heated to 550 °C under argon, (line d) iron oxide coated on A-alumina and heated to 700 °C in air, (line e) iron oxide coated on A-alumina and heated to 1000 °C in air, (line f) iron oxide coated on A-alumina and reduced in the hydrogen at 400 °C for 16 h.

59, 1-butanol 1, and acetonitrile 40 vol %, and the aluminum alkoxide and water concentration was 0.05 and 0.01 mol/L, respectively. The precipitate was washed thoroughly with acetone and dried in a vacuum. Crystallized γ-Al_2O_3 was obtained when heated to 1000 °C.

Sonochemical coating of nanosized iron oxide particles on alumina spheres was carried out in the following way: 400 mg of appropriate alumina was added to 50 mL of Decalin in a sonication cell connected to the sonicator under flowing argon, and then 1 mL of filtered iron pentacarbonyl was added. Prior to sonication, argon gas was bubbled for 1 h, preventing possible oxidation of iron from dissolved oxygen. The irradiation of iron carbonyl and alumina spheres was carried out by employing a high-intensity ultrasonic Ti-horn (20 kHz, 100W/cm^2) under 1.5 atm of argon at 0 °C for 3h. The product was washed thoroughly with hexane. For comparison, three kinds of alumina were used in the sonication. They are as-prepared, calcined at 700 and 1000 °C alumina, and denoted as A-, B-, and C- alumina, respectively.

X-ray diffraction(XRD) measurements were carried out on a model 2028(Rigaku) diffractometer (Cu Kα). The air-sensitive samples were covered with a layer of collodion in the inert atmosphere of a glovebox prior to XRD measurement in order to prevent from oxidation. The observation of particle morphology and their adherence to alumina was conducted on a JEOL-JEM 100SX microscope. DSC studies were carried out on a Mettler DSC 30 by using argon as the carrying gas. Infrared spectra were recorded employing a Nicolet 410 FTIR spectrometer by a KBr disc method. Mössbauer measurements were carried out at room and liquid nitrogen temperatures, using a conventional constant acceleration spectrometer with a ^{57}Co in Rh matrix. Calibration was performed using a 25 μm thick natural foil; the isomer shift values are referred to α-Fe. Magnetization measurements were conducted by employing a Quantum Design MPMS squid magnetometer on accurately weighed samples packed in a gelatin capsule under argon.

III. Results and Discussion

Figure 1 displays the XRD patterns of as-prepared alumina and its iron coating products. It is clearly indicated that as-prepared alumina and its as-prepared sonication product possess

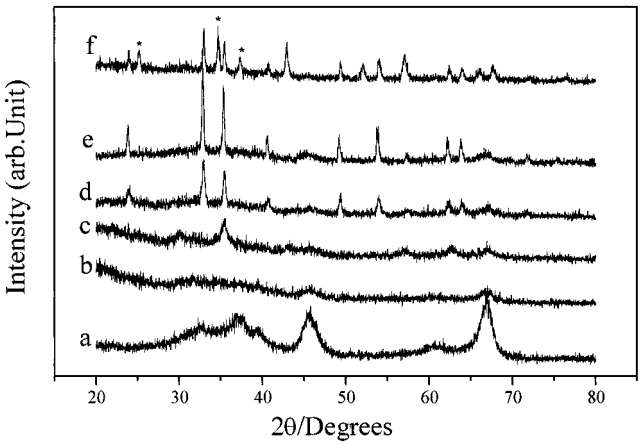

Figure 2. XRD patterns of (line a) alumina heated at 1000 °C, (line b) as-prepared sample of iron oxide coated on C-alumina, (line c) iron oxide coated on C-alumina and heated to 400 °C under argon, (line d) iron oxide coated on C-alumina and heated to 550 °C under argon, (line e) iron oxide coated on C-alumina and heated to 700 °C in air, iron oxide coated on C-alumina and heated to 1000 °C in air.

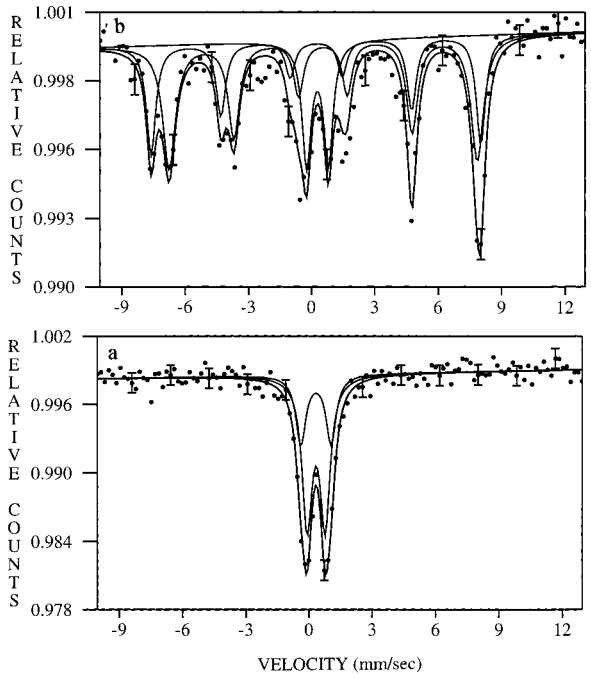

Figure 3. Mössbauer spectra of (part a) as-prepared iron oxide coated on A-alumina and measured at 90 K, (part b) iron oxide coated on A-alumina, heated to 400 °C under argon, and measured at room temperature.

an amorphous nature (Figure 1a). The amorphous nature was further confirmed by our electron diffraction measurements, which show only a diffuse ring. The Mössbauer measurement also confirms the amorphous nature, as illustrated in Figure 3, line a, exhibiting only a broad doublet at liquid nitrogen temperature and indicating that no long-range ordering exists. This broad doublet may be fitted by computer simulation with two or three quadruple doublets corresponding to various forms of iron oxides or hydroxides in the amorphous form. Artificially, it is fitted with two sub-spectra. The parameters of the subspectrum are listed in Table 1, characteristic of a trivalent iron cations. In the original sonochemical preparation of nanometer Fe_2O_3, Cao et al.[15] also reported that the particles with an average size ca. 25 nm are amorphous.

After heating the above as-prepared iron oxide coated on A-alumina at 400 °C in argon, X-ray diffraction peaks appear

TABLE 1: Mössbauer Spectra Parameters for the Samples of Iron Oxide Coated on A-Alumina[a]

sample	T (K)	δ/Fe (mm/s)	ΔE_q (mm/s)	H (KOe)
as-prepared	90	0.44(3)	0.86(2)	
		0.44(1)	1.44(3)	
400 °C-heated	300	0.53(4)		459(2)
		0.22(2)		492(2)
		0.27(2)	1.03	

[a] δ is the isomer shift(relative to α-Fe), ΔE_q the quadrupolar splitting, H the hyperfine field.

and are assigned to γ-Fe_2O_3 or Fe_3O_4 according to ASTM card 19−692 for Fe_3O_4 and 24-81 for γ-Fe_2O_3 (Figure 1, line b). The XRD patterns of these two oxides are almost identical. Because of the poor crystalline nature of our samples, it was difficult to determine whether the heated material is Fe_2O_3 or Fe_3O_4, or their mixture. To further determine this, the Mössbauer spectrum at room temperature was measured (Figure 3, part b). The spectrum consists of the superposition of two sextets and a central doublet. The doublet is fitted with one subspectrum with an isomer shift of 0.27 mm s^{-1}, and a quadrupolar splitting of 1.03 mm s^{-1}, characteristic of γ-Fe_2O_3. The fitting of the second subspectrum yields the characteristic parameters of Fe_3O_4[16] (Table 1). In the structure of Fe_3O_4 (magnetite), Fe^{2+} cations occupy sites in A, whereas Fe^{3+} cations occupy sites in A and B. But because of the fast electron hopping between Fe^{2+} and Fe^{3+} cations, only an averaged spectrum is produced and hence its quadrupolar splitting effect cannot be observed. The quantitative amount of the two phases corresponding to the doublet and sextets were estimated from their spectral area. According to the calculation, the content of γ-Fe_2O_3 is 18% whereas that of Fe_3O_4 is 72%. Thus the coated sample heated at 400 °C is a mixture of γ-Fe_2O_3 and Fe_3O_4. The steps by which this mixture is obtained are as follows. The as-prepared material is perhaps a mixture of iron (III) oxide, iron (III) oxyhydroxide, and iron (III) hydroxide. Heating this amorphous mixture to 400 °C in argon can lead to the decomposition of precursor, removal of the oxygen, and finally the formation of Fe_3O_4. Finding 18% of γ-Fe_2O_3 in the final mixture indicates that this process has not been completed under the reaction conditions. In addition, we cannot completely rule out the possibility that the Fe_3O_4 was reoxidized in the process of sample transfer, because Fe_3O_4 can transform rapidly to γ-Fe_2O_3 at temperatures as low as 100 °C in the presence of air.[17]

For B-alumina heated at 700 °C in air for 4 h and its coated products, a similar appearance to the sample coated on A-alumina was observed. The as-prepared sample coated on B-alumina is also found to be X-ray amorphous. After the sample was heated 400 °C in argon, some peaks assigned by XRD measurements as Fe_2O_3 or Fe_3O_4 were observed. Alumina heated at 1000 °C and its coated samples (Figure 2) also possess similar X-ray diffraction patterns, except that, in addition, we observe the appearance of γ-Al_2O_3 peaks(Figure 2, lines a and b). It is also found that, after coating, the peak intensity assigned to γ-Al_2O_3 decreases, obviously due to iron oxides capping the outside surface of alumina spheres.

TEM images of different samples are shown in Figure 4. Figure 4, part a, presents the TEM image of iron oxide coated on A-alumina, and Figure 4, part b, is its magnified image. It is clearly shown that the alumina surface is almost fully covered by iron oxides. Most of the iron oxide particles are adhered to the surface of alumina spheres, but individual particles cannot be easily discernible; they look like a dense cloud covering the alumina core. After heated to 400 °C under argon for 4 h, the iron oxide particles are greater in size due to their sintering. They are also better resolved and possess a relatively regular spherical shape with an average radius of 10−20 nm. Apparently, the heating at 400 °C promoted the coating of iron oxide on the alumina core. After reduction under hydrogen at 400 °C for 16 h, most of coated particles have grown in size and only α-Fe is identified by XRD (Figure 1, line f). For samples of iron oxide coated on B-aluminas, a similar phenomenon is observed, except that a lesser amount of iron oxide particles is adhered to the alumina surface, compared to iron oxide coated on A-alumina. In contrast to the above two samples, the iron oxide coated on crystallized alumina (C-alumina) is an agglomerate of small particles with a size distribution of 1−10 nm, and most of the iron oxide particles are not anchored to the alumina spheres. Obviously, the coating effect is mainly determined by the reactivity of the alumina surface toward the iron oxide, and the surface reactivity of alumina varies with the heating temperatures. The highest reactivity was observed with the as-prepared alumina having an amorphous structure.

Figure 5 shows DSC curves of as-prepared sonication products. Figure 5, line a, presents the DSC curve of as-prepared iron oxide coated on A-alumina, Figure 5, line b, on B-alumina, and Figure 5, line c, on C-alumina. The broad endothermic peak centered at ca. 150 °C in all three curves is attributed to the desorption of contaminants such as solvent molecules and the carbonyl precursor from the surface of the product. The large exothermic peak in the range of 200−380 °C corresponds to the crystallization of amorphous iron oxide to γ-Fe_2O_3. This is consistent with our previous results[15,18] and interpretation, as well as with the above XRD and Mössbauer results, in which, after being heated to 400 °C in argon, a mixture of crystallized γ-Fe_2O_3 and α-Fe_2O_3 was observed. At the same time, it seems that this crystallization peak shifts to a low temperature with the increase of heat-treating temperature of the alumina substrate. For iron oxide coated on A-alumina (Figure 5, line a), a sharp and small exothermic peak at ca. 370 °C is observed, which is the highest temperature peak among the three sonication products in above-mentioned temperature region. This may be related to the different nature of the interaction between the as-deposited material and the various alumina substrates. The stronger the chemical interaction, the higher will be the crystallization temperature.

In addition, differences in the DSC spectra in the temperature range of 400−550 °C should also be noted. The Figure 5, line a, shows only a straight plain curve in this temperature range (a very broad and small peak is also recognizable), while in Figure 5b a small and broad exothermic peak is detected. In contrast to the above two samples, a comparatively large exothermic peak is observed for iron oxide coated on C-alumina (Figure 5, line c). It is well-known that the transformation of γ-Fe_2O_3 or Fe_3O_4 to α-Fe_2O_3 occurs in this temperature region.[19] Taking into account the fact that the amount of iron oxide adhered tightly to the alumina surface is different in the above three samples, it is reasonable to divide the state of coated iron oxide into two parts: (1) the adhered iron oxide, which is connected tightly to the alumina core, and (2) the dissociated or unadhered iron oxide, which is floating in the interparticle space of alumina spheres. Our interpretation of the differences in the DSC spectra in the 400−550 °C is similar to that proposed for the crystallization temperatures. Namely, the transition temperature of the γ-Fe_2O_3 to α-Fe_2O_3 phase for the tightly adhered iron oxide occurs at higher temperatures than for the dissociated and unadhered iron oxide. In other words, the unadhered iron oxide should exhibit a $\gamma \rightarrow \alpha$ conversion temperature similar to that of pure iron oxide.

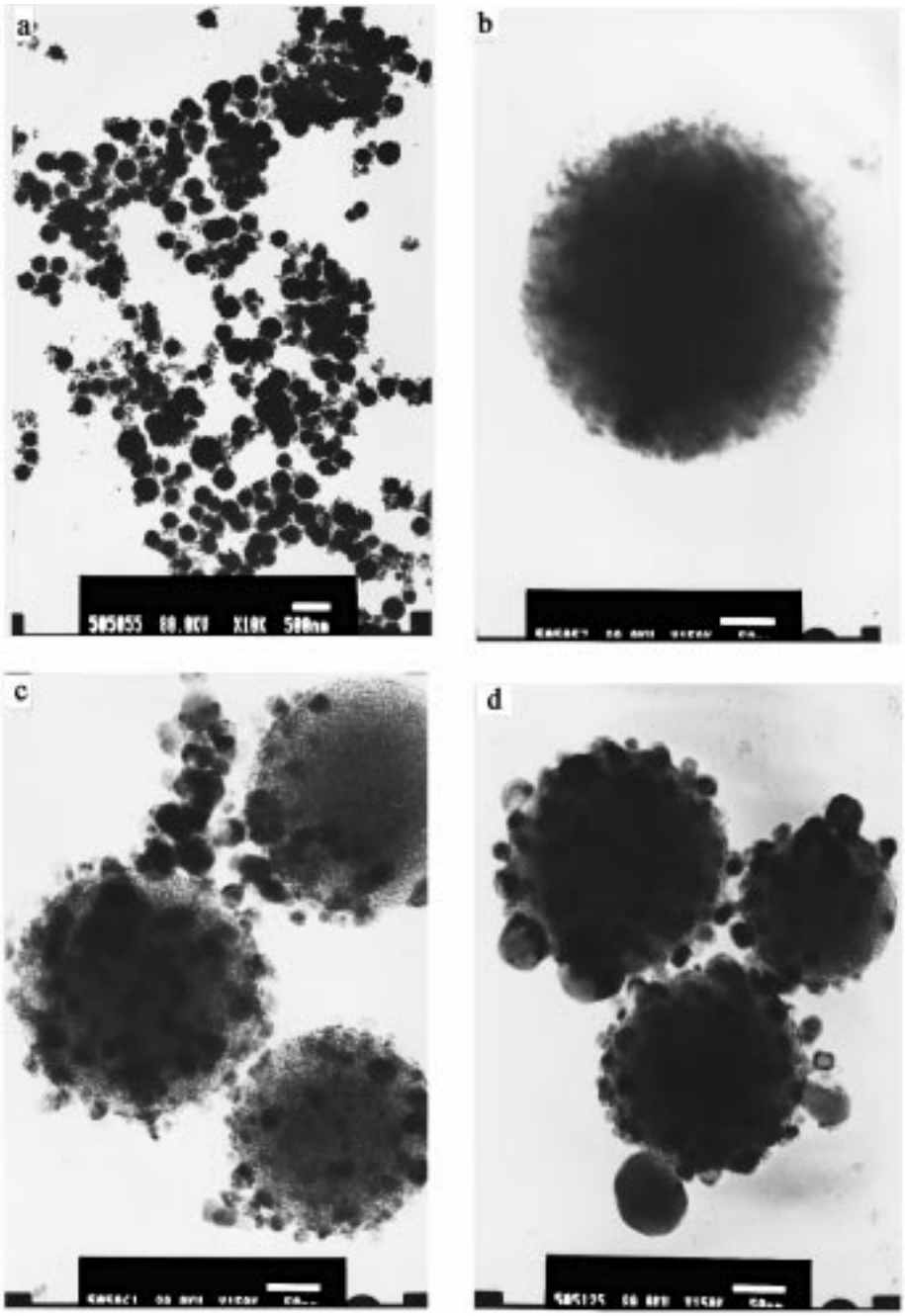

Figure 4. TEM micrographs of (part a) as-prepared iron oxide coated on A-alumina, (part b) magnified picture of part a, (part c) iron oxide coated on A-alumina and heated at 400 °C, (part d) iron oxide coated on A-alumina and reduced at 400 °C in hydrogen for 16 h.

To confirm this, two investigations were carried out. One, in which a pure amorphous Fe_2O_3 sample was prepared following Cao's method.[18] Its DSC curve is shown in Figure 5, line d. A similar but larger exothermic peak compared with Figure 5, line c, is observed. As a second check, the as-prepared sonication products of iron oxide coated on A- and C-alumina were heated to 550 °C under argon, and their XRD and magnetization measurements were examined. The XRD patterns are shown in Figure 1, line c, and Figure 2, line d, respectively. From Figure 1, line c, it can be confirmed that γ-Fe_2O_3 is the main phase of iron oxide coated on A-alumina, and α-Fe_2O_3 is a minor phase (the XRD peak of the minor α-Fe_2O_3 phase is marked with an asterisk at $2\theta = 33.0°$ and $d = 2.71$ Å). In contrast to the above sample, the XRD pattern of iron oxide coated on C-alumina after being heated to 550 °C under argon shows the characteristic peaks of α-Fe_2O_3. It is known that γ-Fe_2O_3 is a ferrimagnetic material and α-Fe_2O_3 a weakly ferromagnetic or antiferromagnetic material.[19] Thus, it is expected to see a dramatic difference in magnetization behavior between the above two samples heated at 550 °C. Figure 6 shows their magnetization curves. It is seen that the samples coated on A-alumina and heated at 550 °C(Figure 6, line b) possesses a much higher magnetization than the sample coated on C-alumina(Figure 6, line a), indicating the transformation of α-Fe_2O_3 in the latter sample.

The mechanism of the $\gamma \rightarrow \alpha$ phase transformation is also known to be dependent on the particle size. The proposed mechanism for this transformation of small particles (<15 nm) is that of a chain mechanism which involves recrystallization of up to 100 particles to form single α-Fe_2O_3 flakes of ca. 40−70 nm.[20] Obviously, the strong interaction between adhered iron oxide and alumina can hinder this kind of gathering and recrystallization of iron oxide particles on an alumina surface.

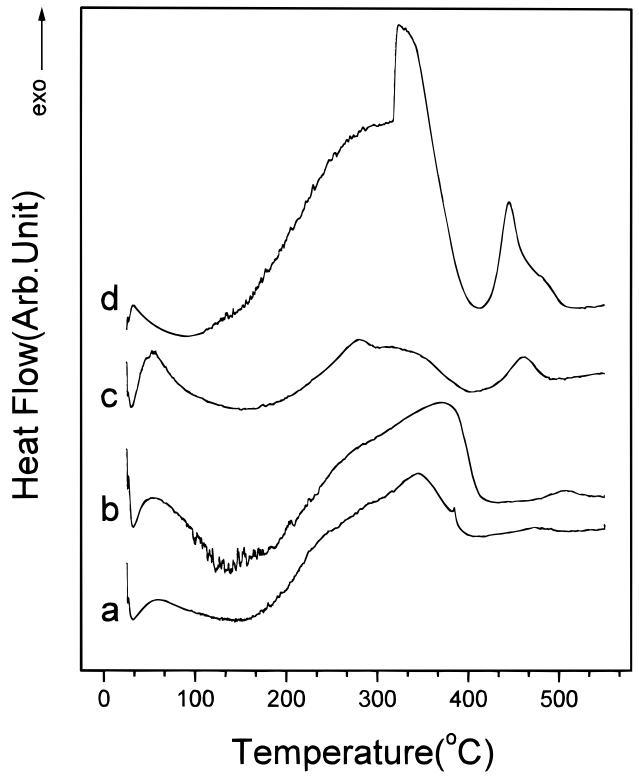

Figure 5. DSC curves of (line a) as-prepared iron oxide coated on A-alumina, (line b) as-prepared iron oxide coated on B-alumina, (line c) as-prepared iron oxide coated on C-alumina, (line d) iron oxide prepared by the sonication of $Fe(CO)_5$ under air.

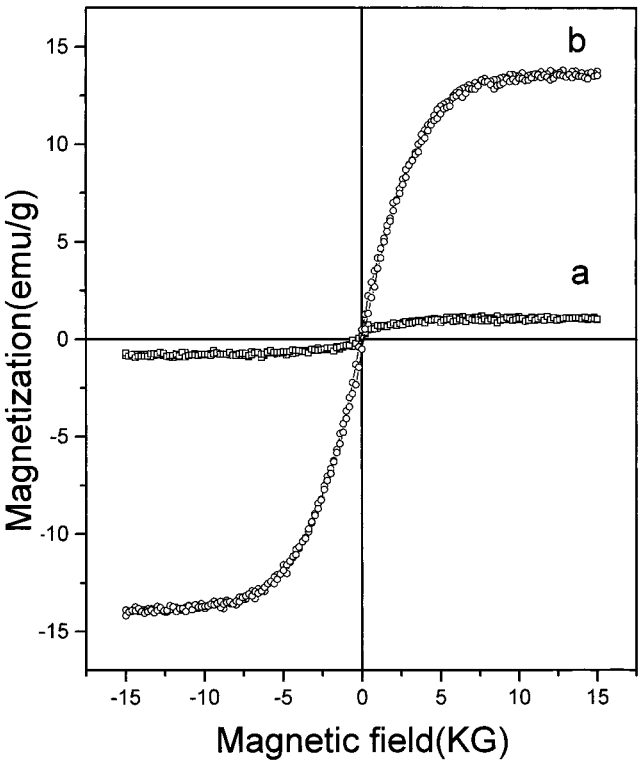

Figure 6. Magnetic curves of samples coated on A-and C alumina and heated to 550 °C in argon: (a) on C-alumina, (b) on A-alumina.

The strong interaction may originate from the incorporation of Al^{3+} into the subsurface defects in iron oxide matrix, which can elevate the transformation temperature.[21]

The interaction can be observed more directly by the combination of TEM and XRD measurements. Figure 7, part a, is an image of iron oxide coated on A-alumina and heated to 550 °C. The unadhered iron oxide particles in the middle of picture (marked with an arrow) have grown to ca. 50−100 nm, whereas the adhered iron oxide particles remain small, having sizes of ca. 10−30 nm. According to the above discussion, the unadhered particles possess a α-Fe_2O_3 structure and is the minor phase, while the adhered particles possess a γ-Fe_2O_3 structure as the main phase. For the sample coated on A-alumina and heated at 700 °C, TEM image shows that most of the adhered iron oxide particles are still recognizable and separated from each other on the surface of alumina spheres. XRD shows that it is a mixture of α-Fe_2O_3 and γ-Fe_2O_3. The presence of γ-Fe_2O_3 in this sample is confirmed by comparing the intensity of diffraction peaks at $2\theta = 33.0°$($d = 2.71$) and $2\theta = 35.6°$($d = 2.52$). Pure α-Fe_2O_3 should exhibit its strongest peak at $2\theta = 33.0°$(d = 2.71), whereas the above sample exhibits its strongest peak at $2\theta = 35.6°$($d = 2.52$) due to the overlapping of diffraction peaks of α-Fe_2O_3 and γ-Fe_2O_3 at this position. The complete transformation of $\gamma \rightarrow \alpha$ can be further confirmed by the sample which is heated to 1000 °C, in which the strongest peak is observed at $2\theta = 33.0°$ (Figure 1, line e). Most surprisingly, it is found that in the sample heated to 1000 °C, the alumina submicrospheres are completely broken to pieces, and the size of iron oxide particles has become larger than 150 nm (Figure 7, line c). Obviously, the iron oxide particles are connected very tightly to the alumina cores. At high temperatures, the strong attractive force between iron oxide particles has caused the assembly of iron oxide, even at the cost of the complete damage of alumina spheres or breakdown of some Al−O bonds. According to the above facts, we may conclude that iron oxide and alumina are not connected through a physical interaction, but rather through a strong chemical bond, such as Al−O−Fe. The XRD pattern (Figure 1, line e) of this sample shows the formation of α-Al_2O_3 and α-Fe_2O_3 compared to ASTM cards 10-173 and 33-664, respectively. Meanwhile, three newly formed peaks are observed at $2\theta = 25.2°$($d = 3.54$), 34.70°($d = 2.59$), and 37.2°($d = 2.24$), which can neither simply be assigned to α-Al_2O_3 nor be α-Fe_2O_3. We believe they may originate from a new kind of bulk phase or surface phase compound.

To observe the interaction between iron oxide and alumina more clearly, the sample of iron oxide coated on C-alumina was also heated to 1000 °C for 4 h. Its TEM image (Figure 7, part d) clearly shows the damage to the alumina spheres; however, the contour of the alumina sphere is still discernible in the picture. The comparatively slight damage is due to the fact that in this sample the interaction between the iron oxide and the alumina substrate is the weakest. XRD patterns (Figure 2, line f) show that its main phases are α-Al_2O_3 and α-Fe_2O_3, and in addition, three new peaks at $2\theta = 25.2°$($d = 3.54$), 34.7°-($d = 2.59$), and 37.2°($d = 2.24$) are also been observed, whereas, pure substrate alumina heated at the same temperature possesses the structure of γ-Al_2O_3, as identified by XRD (Figure 2, line a), and all particles have a regular shape and comparably smooth surface. These results indicate that the transformation of γ-Al_2O_3 to α-Al_2O_3 in the coated sample is induced and catalyzed by α-Fe_2O_3. Furthermore, this kind of "induction" should not only be limited to the surface or to the subsurface. Otherwise, most of the alumina would remain the structure of γ-Al_2O_3. The evolution of the phase change has been detected even at lower temperatures and a relatively longer heating time. This is demonstrated in Figure 7, part c. In this image, the as-prepared sample of iron oxide coated on C-alumina was calcined at 700 °C for 48 h. It is very clearly shown that iron oxide particles

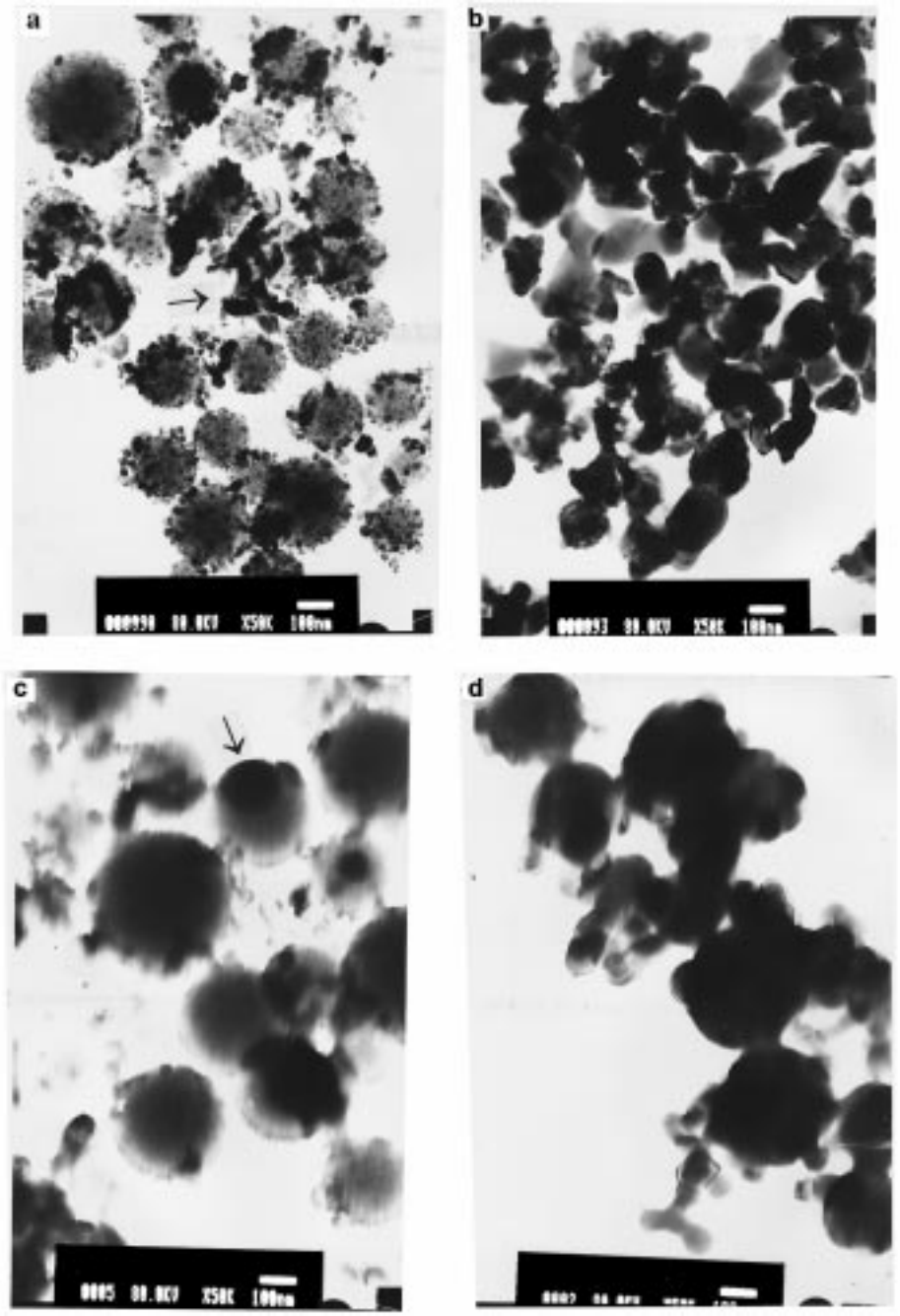

Figure 7. TEM micrographs of (part a) iron oxide coated on A-alumina and heated at 550 °C in argon, (part b) iron oxide coated on A-alumina and heated at 1000 °C in air for 4 h, (part c) iron oxide coated on C-alumina and heated at 700 °C in air for 48 h, (part d) iron oxide coated on C-alumina and heated at 1000 °C in air for 4 h.

are incorporated into the alumina spheres (marked as an arrow in picture), but the boundary between iron and alumina is still discernible. The sintering of iron oxide particles on the alumina surface indicates that the phase transformation of iron oxide is indeed following the chain mechanism, and the interaction between iron oxide and the alumina substrate is very strong. Otherwise, the attraction forces among iron oxide particles would lead iron oxide particles to leave the alumina surface. Meanwhile, a slight obscure boundary structure between iron oxide and alumina reveals a possible diffusion of iron ions into the cations defects at the interface of alumina and the strong interaction between iron oxide and alumina.

The Fe^{3+} and Al^{3+} ions have a very similar radius (the radius for Fe^{3+} is 0.55Å, and that of Al^{3+} is 0.54 Å, in an octahedral coordination),[22] so it is not surprising, that, in the process of calcination, Fe^{3+} cations can incorporate into the octahedral vacancies on the surface or subsurface of Al_2O_3 substrate to form a kind of solid solution at the interface. This phenomenon is reported by a number of authors.[23−27] For example, Carbucicchio[25] observed the formation of the surface solid solution of aluminum and iron oxide on the surface of alumina heated at 1100 °C by Mössbauer spectra. Vaishnava et al.[26] observed the same phenomenon for η-Al_2O_3, and Vuurman[27] for γ-Al_2O_3. So the three newly observed peaks in Figure 1, line e, and Figure 2, line f, should be assigned to the newly formed surface solid solution. The newly formed surface solid solution should be different from the compound of aluminate spinel $FeAlO_3$ and hercynite $FeAl_2O_4$ in structure, because these compounds are formed only above 1300 °C.[28−30] The formula of the surface solid solution can be written in the form of $Al_{2-x}Fe_xO_3$, in which

TABLE 2: Phase Composition of Alumina-Coated Samples Heated at Different Temperatures

heating temperature (°C)	on A-alumina	on C-alumina
400	γ-Fe_2O_3 + Fe_3O_4 + amorphous Al_2O_3	γ-$Fe_2O_3$$^+$ or Fe_3O_4 + γ-Al_2O_3
550	γ-Fe_2O_3 + trace α-Fe_2O_3 + amorphous Al_2O_3	α-Fe_2O_3 + γ-Al_2O_3
700	γ-Fe_2O_3 + α-Fe_2O_3 + amorphous Al_2O_3	α-Fe_2O_3 + γ-Al_2O_3
1000	α-Fe_2O_3 + α-Al_2O_3 + $Al_{2-x}Fe_xO_3$ (at the interface)	α-Fe_2O_3 + α-Al_2O_3 + $Al_{2-x}Fe_xO_3$ (at the interface)

the mother structure of Al_2O_3 or Fe_2O_3 is remained as discussed herein. Table 2 presents a summary of our results and the assignment of the phase composition as a function of temperature.

In fact, not only are Fe^{3+} ions able to incorporate into the defects of Al_2O_3, as reported by Sidhu,[21] but trace amounts of Al^{3+} can also diffuse into the Fe_2O_3 matrix. The most interesting phenomena, as observed in our experiments, is that at low temperatures the amorphous alumina substrate can stabilize the γ-Fe_2O_3 structure, and at high temperatures, the Fe^{3+} in alumina can induce the formation of α-Al_2O_3. Naturally, it is not unreasonable to assume that the atomic arrangement at the interface should closely reflect the stable structure of the two bordering components. For example, at low temperatures, the structure of alumina is far from the structure of its α-phase, so the arrangement of Al^{3+} in the amorphous form can induce the arrangement of Fe^{3+} in the interface monolayer of Fe_2O_3, and this monolayer can further induce the arrangement of subsurface Fe^{3+} ions in the second layer, and so forth. In this way, the inducement can be conducted layer by layer, and appears to be a long-range action. At high temperatures, as mentioned above, because of a very close ion radius for Fe^{3+} and Al^{3+} in octahedral coordination, the diffusion of Fe^{3+} ions into the octahedral vacancies on the Al_2O_3 surface becomes possible, so that finally α-Fe_2O_3 can induce the formation of α-Al_2O_3.

Over the past 40 years, aluminas of various forms have been considered to be one of the metal oxide model systems that has been most extensively studied by Infrared spectroscopy. This is because alumina is a commonly used material for catalysis.[12] Despite a wealth of information, obtained by IR studies about alumina structure, many questions are still open, and the details of surface structure are still lacking. The results we present will use only the commonly agreed upon knowledge of IR spectra as a tool in helping to understand the structure of our samples and the interaction between alumina and iron oxide.

Figure 8 and 9 show IR spectra of samples coated on A- and C-alumina, respectively. The absence of a peak at 2000−2100 cm^{-1} indicates the absence of iron carbonyl from the alumina surface after sonication and washing.[31] The IR spectra below 1000 cm^{-1} usually reflect the vibration of the M−O bond (here M represents a metallic element). As reviewed by Morterra,[13] it is known that the stretching vibration of Al−O for the octahedrally coordination of Al ions is in the range of 600−750 cm^{-1}, while the Al−O vibration in tetrahedraly coordinated Al ions is in the range of 750−900 cm^{-1}. It is seen from Figures 8 and 9, that all samples of iron oxide coated on A- and C-alumina and heated below 1000 °C have broad peaks above 750 cm^{-1}, revealing the presence of tetrahedrally coordinated Al ions. After heating to 1000 °C (Figures 8, line f, and Figure 9, line f), only peaks at 668 cm^{-1} and at lower wavenumbers are observed, reflecting on the disappearance of tetrahedrally coordinated Al^{3+} ions and the formation of octahedrally coordinated Al^{3+} ions. This is in good agreement with the above XRD results, in which only α-Al_2O_3 was observed after heating to 1000 °C.

Special attention is paid to the change in the energy region below 500 cm^{-1}, because IR absorption bands for Fe−O bond at higher wavenumbers are overshadowed by the Al−O bands.

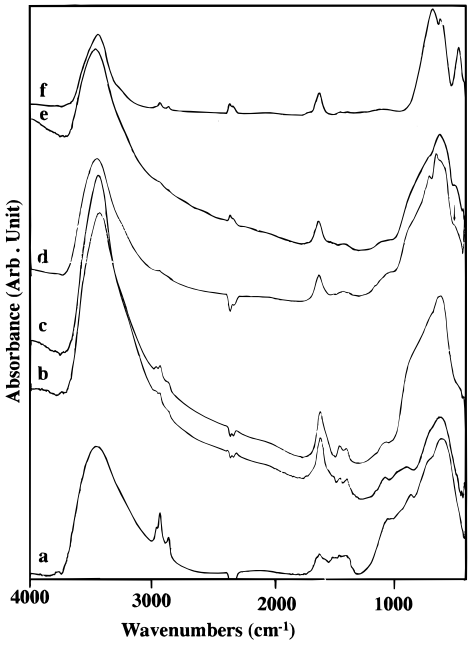

Figure 8. Infrared spectra of (line a) as-prepared alumina, (line b) as-prepared sample of iron oxide coated on A-alumina, (line c) iron oxide coated on A-alumina and heated to 400 °C under argon, (line d) iron oxide coated on A-alumina and heated to 550 °C under argon, (line e) iron oxide coated on A-alumina and heated to 700 °C in air, (line f) iron oxide coated on A-alumina and heated to 1000 °C in air.

The band at ca. 450−480 cm^{-1} is assigned to the Fe−O bond vibration in α-Fe_2O_3[19]. The band peaked at 474 cm^{-1}, for iron oxide coated on C-alumina, appears only after the sample is heated to 550 °C (Figure 9, line d). The relative intensity of this peak is increased with the increase of the heating temperature, indicating the formation of α-Fe_2O_3 and the increase of its crystallinity. This is consistent with the above XRD measurements. In samples coated on A-alumina, a similar phenomenon can be observed. In Figure 8, line d (heated to 550 °C), a small shoulder peaked at 480 cm^{-1} is discerned (marked with an arrow), which coincides with the appearance of a minor α-Fe_2O_3 phase observed by XRD. After being heated to 1000 °C, a sharp peak centered at 453 cm^{-1} is observed, which is indicative of an α-Fe_2O_3 phase.

Figures 8 and 9 show that the frequency of the Fe−O stretching vibration in α-Fe_2O_3 decreases, as the heating temperature is increased. This can be attributed to the increase of alumina substitution in α-Fe_2O_3 lattices[34] at an elevated temperature as discussed above.

Brenner et al.[4] carried out an investigation on the reaction between Al_2O_3 surface hydroxyls and zerovalent metals formed by the thermal decomposition of the various adsorbed metal carbonyls. The reaction can be described by the following equation:

$$M(CO)_j + n(\sigma\text{-OH}) \rightarrow (\sigma\text{-O}^-)_n M^{n+} + (n/2)H_2 + jCO \quad (1)$$

This means that the interaction between the transition metal element and the Al_2O_3 substrate is through the hydroxyls on

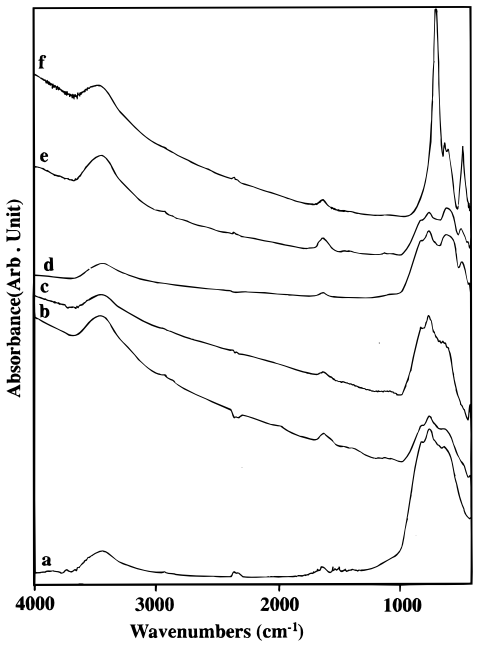

Figure 9. Infrared spectra of (line a) C-alumina heated at 1000 °C, (line b) as-prepared sample of iron oxide coated on C-alumina, (line c) iron oxide coated on C-alumina and heated to 400 °C under argon, (line d) iron oxide coated on C-alumina and heated to 550 °C under argon, (line e) iron oxide coated on C-alumina and heated to 700 °C in air, (line f) iron oxide coated on C-alumina and heated to 1000 °C in air.

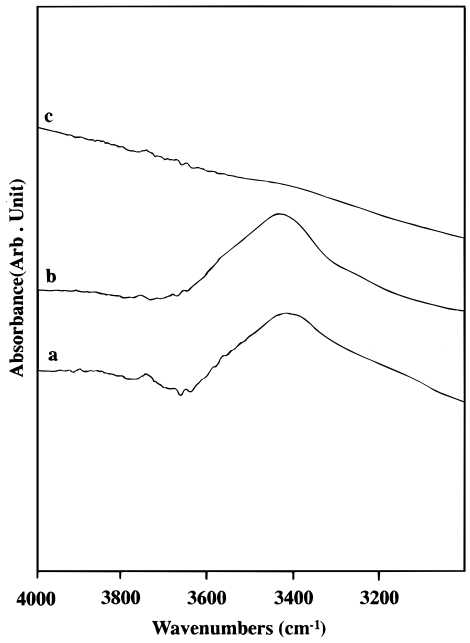

Figure 10. Difference Infrared spectra of (line a) as-prepared iron oxide on A-alumina−A-alumina, (line b) as-prepared iron oxide on B-alumina−B-alumina, (line c) as-prepared iron oxide on C-alumina−C-alumina.

the surface, so the observance of IR spectra of hydroxyls should provide some details of this interaction. As reported by many authors,[13] the fundamentals of the O−H stretching vibrations of the surface hydroxyl groups of oxides, such as silica and alumina, can be observed in the region of 3000−4000 cm^{-1}. In general, there are three types of OH groups on the alumina surface, namely, the adsorbed water in the form of undissociated coordinated H_2O, the O−H groups of H-bonding type and isolated OH groups (free of the H-bonding).[12,13] The position of isolated OH bands appears in the region of 3600−3800 cm^{-1}, while H-bonded OH groups absorb below 3600 cm^{-1}. Though there are many disputes on the origin and assignment of isolated OH groups, it is assigned to the absorption at 3775 cm^{-1}, which is the most active vibration in catalysis.[12]

In Figure 8 and 9, it is seen that the fine structure of the peaks above 3000 cm^{-1} is not resolved, and it is difficult to distinguish individual bands. This may be related to the formation of iron oxyhydroxide in the sonication as mentioned above, and the re-adsorbed moisture on samples in the process of sample handling. From Figure 8, lines a and b, it is seen that, for samples coated on A-alumina, there is a slight decrease in intensity for bands above 3600 cm^{-1}, when compared with the absorption intensity of the bare alumina (non sonicated). There is almost no change in the absorption intensity for iron oxide coated on C-alumina in the same region (Figure 9, lines a and b). This is better depicted in Figure 10 with a difference spectrum, in which the bare alumina spectrum is subtracted from the as-made coated spectrum. For samples coated on A-alumina, a dip peak above 3600 cm^{-1} is observed, while below ca. 3450 cm^{-1} a high-intensity peak is seen (Figure 10, lines a and b). This implies that the sonication causes the isolated OH groups to be consumed. In other words, in the reaction, the isolated hydroxyls react with the iron atoms and form iron oxyhydroxide or iron oxide. This is consistent with the results in the literature claiming that the interaction between a metal and a support surface occurs by the consumption of the alumina's free hydroxyl groups.[35,36] For the sample coated on C-alumina, a plain curve is observed (Figure 10, line c), indicating that no hydroxyl was consumed and that no interaction between the iron and the substrate takes place.

Indeed, as shown by the above TEM image (Figure 7), there are few iron oxide particles adhered to the alumina surface for the sample coated on C-alumina, even after being heated to 550 °C. Recently, Vuurman et al.[36] studied the interaction between deposited nickel and cobalt oxides with γ-Al_2O_3 and found that nickel and cobalt oxides hardly reacted with the hydroxyl groups. They proposed that nickel and cobalt oxides may interact with the surface defects such as Lewis sites (coordinative unsaturated Al^{3+}). However, according to our above observation and discussion, it should be that the iron ions diffuse into Al^{3+} vacancies on alumina surface and that the diffusion occurs only at high temperatures.

Heating the alumina can promote the elimination of OH groups. The concentrations of surface hydroxyl monotonically decrease as the alumina is heated above room temperature.[37] Removal of hydroxyl ions from γ-alumina is thought to be essentially complete at ca. 1200 K, and, in most cases, is irreversible.[13] Evidence suggests that clusters ions, vacancies, and strained Al−O bonds are formed on the alumina surface as a result of the dehydroxylation process and that defect sites are responsible for the enhanced reactivity of heat-treated alumina.[37−39] In our experiments, the crystallized alumina was heated to 1000 °C, where almost no isolated hydroxyls are left, so the interaction between iron and crystallized alumina should be very weak at low temperature. After being heated to a high temperatures, the iron ions can diffuse into the cation vacancies on crystallized alumina surface. As observed in Figures 8 and 9, the Al−O band was strongly perturbed after being heated to more than 700 °C. So there are two types of interaction between iron and alumina. At low temperatures and in the case of A- and B-aluminas, the interaction between iron and the alumina substrate is mainly via free OH groups as a connecting bridge, while at the high temperatures, the interaction is mainly through the diffusion of Fe^{3+} ions into the surface vacancies on alumina substrate.

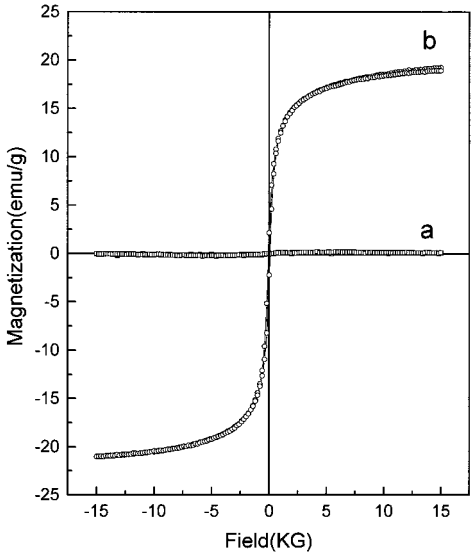

Figure 11. Magnetic curves of samples coated on A-alumina: (line a) as-prepared sample, (line b) heated at 400 °C in argon.

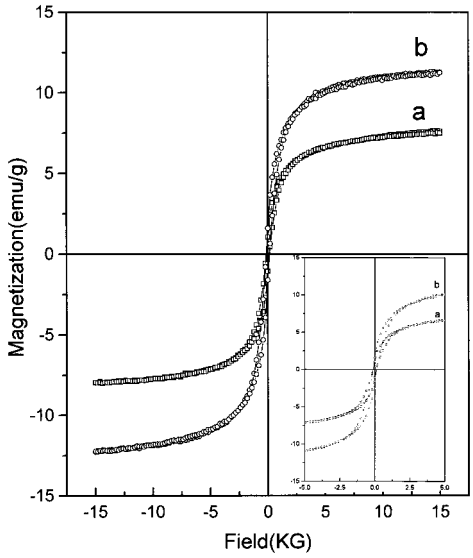

Figure 12. Magnetic curves of samples coated on C-alumina: (line a) as-prepared sample, (line b) heated at 400 °C in argon.

In fact, the interaction through the OH groups between iron and alumina is most probably related to the Lewis sites (near the O^{2-} ions vacancies) on the substrate surface. Recently, in an investigation of the reactions of halomethanes with γ-alumina, Dai et al.[40] found that the formation of Al−X and C−O bonds involves the participation of coordinatively unsaturated Al^{3+} sites. Liu et al.[12] further confirmed that there are three types of surface isolated OH groups on γ-alumina, and each type of hydroxyl is adjacent to one type of Lewis site. The most active OH group at 3775 cm^{-1} is near the strongest Lewis acid sites. Considering the fact that the reaction indicated by eq 1 involves the transfer of electrons, it is not difficult to understand why only isolated OH groups are reactive toward the iron or its carbonyl compound—the adjacent Lewis sites can accept the electron from the iron and promote the reaction. Combining all the above results, we can further deduce that only a part of the isolated OH groups are adjacent to Lewis sites. Otherwise IR bands of isolated OH groups will show a significant change after sonication or deposition.

Figures 11 and 12 show the results of magnetization measurements for samples coated on A- and C-alumina before and after heating at 400 °C. The magnetization is only relative to the unit mass of composite materials. It is seen from Figures 11 and 12 that the heated samples on A- and C-alumina always show a higher magnetization at a given magnetic field than their corresponding as-prepared samples, indicating the sintering and crystallization of amorphous iron products after heating. For samples coated on C-alumina, a very narrow hysterelysis loop is observed, which can be attributed to its easily aggregate property. As discussed in the above, in samples coated on C-alumina, most of the iron product particles are not adhered to alumina surface and are distributed in the interparticle space of alumina spheres, so they are easily to form agglomerate and exhibit the hysterelysis loop. In the case of the samples coated on A-, and B-alumina, most of iron product particles are strongly adhered to alumina surface and keep a very good dispersion state, so the size of iron product is small enough to exhibit the superparamagnetic behavior. It is particularlly noted the difference in the magnetization behaviors of samples before heating. The sample coated on A-alumina shows almost no magnetization, and the sample on B-alumina a slight magnetization, while the sample coated on C-alumina shows a comparatively high magnetization. As discussed above, in the case of A-, and B-alumina, the elemental iron has reacted with the OH groups on the alumina surface and formed a type of Fe−O−Al bond, in which only iron oxide or their oxyhydroxide (the broad feature of its Mössbauer spectra in Figure 3, part a, shows that it is a mixture of several components) was formed and shows a low magnetization. In sample coated on C-alumina, because the absence of enough OH groups, we believe that part of elemental iron is remained, so it exhibits a high magnetization.

Up to now, we have still not addressed the question about the origin of the oxygen responsible for the oxidation of iron coated on C-alumina, because γ-Fe_20_3 or Fe_3O_4, or their mixture were observed after being heated to 400 °C (Figure 2, line c). The origin of the oxygen in this case is mainly the free OH groups on the A-, and B-alumina surface. However, to C-alumina, because all of the isolated OH groups are eliminated, the question remains open. In a similar case, Ramesh[6] observed the formation of α-Fe and a small amount of Fe_3O_4 on highly dehydrated silica and suggested that surface oxygen can form a moderately covalent tie with elemental iron (in the from of Fe−O−Al). But in our TEM experiments for samples coated on C-alumina, we find that most of iron oxide particles are not adhered to the alumina surface even after being heated to 550 °C. So we believe that the oxygen may partially come from physically adsorbed water on C-alumina surface because it was heated and cooled in the air. The oxidation of the rest elemental iron may be surface oxygen of alumina. The evidence for the existence of water molecules is observed in the appearance of the 1636 cm^{-1} bending vibration and the symmetric and antisymmetric stretching vibrations in all spectra and after all treatments (see Figures 8−9). In the sonication process, the physical absorbed water may easily desorb from the alumina surface and react with ultrafined particles of element iron. In contrast, in the presence of isolated OH groups, because it is difficult to remove the isolated OH groups from the alumina surface and because of their highly reactivity toward element iron, the covalent bond Fe−O−Al is easily formed and the connection position further becomes a nucleation center. On the surface of alumina, the distribution of the isolated OH groups near Lewis sites should be scattered in a random way, so in TEM images we can observe the separate small iron oxide spheres on alumina surface after sonication.

IV. Conclusions

Studies of coating iron oxide on alumina treated at different temperatures show different coating behaviors. The optimum coating is observed on as-prepared amorphous alumina, in which most of iron oxide particles are tightly adhered to alumina spheres; while in the sample coated on crystalline alumina heated to 1000 °C, most of the iron oxide particles are separate from the alumina spheres.

The strong interaction between adhered iron particles and alumina substrate can hinder the transformation of γ-Fe_2O_3 to α-Fe_2O_3 even at temperatures higher than 700 °C; conversely, the presence of α-Fe_2O_3 can induce the formation of α-Al_2O_3 at high temperatures.

In the samples of iron oxide coated on amorphous alumina, the interaction is first via the reaction of iron with isolated OH groups on the alumina surface, while at high temperatures, the iron ions can incorporate into the cation vacancies in alumina and form a solid solution of $Al_{2-x}Fe_xO_3$ at the interface.

Acknowledgment. A. Gedanken thanks the Ministry of Science and Technology for supporting this research through a grant for infrastructure. Dr. Ziyi Zhong thanks the Kort Scholarship foundation for supporting his postdoctoral fellowship. The authors thank Professor M. Deutsch, Department of Physics, for extending the XRD facility, and Dr. Shifra Hochberg for editorial assistance.

References and Notes

(1) Segal, D. *Chemical Synthesis of Advanced Ceramic Materials*; Cambridge University Press: Cambridge, 1989.

(2) Yanagida, H.; Koumoto, K,; Miyayama, M. *The Chemistry of Ceramics*; John Wiley & Sons: New York, 1996.

(3) Tsyganenko, A. A.; Mardilovich, P. *J. Chem. Soc., Faraday Trans.* **1996**, *92*, 4843.

(4) Hucul. D. A.; Brener, A. *J. Phys. Chem.* **1981**, *85*, 496.

(5) (a) Suslick, K. S., Ed. *Ultrsound: Its chemical, Physical and Biological Effects*; VCH: Weinheim, 1988. (b)Susclick, K. S.; Choe, S. B.; Cichowlas, A. A.; Grinstaff, M. W. *Nature* **1991**, *353*, 414.

(6) Ramesh, S.; Prozorov, R.; Gedanken, A. *Chem. Mater.* **1997**, *9*, 2996.

(7) Ramesh, S.; Koltypin, Y.; Prozorov, R.; Gedanken, A. *Chem. Mater.* **1997**, *9*, 546.

(8) Ramesh, S.; Cohen, Y.; Prozorov, R.; Shafi, K. V. P. M.; Aurbach, D.; Gedanken, A. Organized silica microspheres carrying magnetic cobalt nanoparticles as a basis for "tip arrays" in magnetic force microscopy. *J. Phys. Chem. B.* Submitted for publication.

(9) Dormann, J. I.; Djega-Mariadasson, C.; Jove, J. J. *Magn. Magn. Mater.* **1992**, *104*, 1576.

(10) Djega-Mariadasson, C.; Dormann, J. I.; Nogues, M.; Viller, G.; Sayouri, S. *IEEE Trans. Magn.* **1990**, *26*, 1819.

(11) Leslie-Peleky, D. L.; Rieke, R. D. *Chem. Mater.* **1996**, *8*, 1770.

(12) Liu, X.; Truitt, R. E. *J. Am. Chem. Soc.* **1997**, *119*, 9856.

(13) Morterra, C. C.; Magnacca, G. *Catal. Today* **1996**, *27*, 497.

(14) Ogihara, T.; Nakajima, H.; Yanagawa, T.; Ogata N.; Yoshida, K.; Matsushita, N. *J. Am. Ceram.* **1991**, *74*, 2263.

(15) Cao, X.; Koltypin, Y.; Prozorov, R.; Kataby, G.; Gedanken, A. *J. Mater. Chem.* **1997**, *7*, 2447.

(16) Banerjee, S. K.; O'Relly. W.; Johnson, A. H. *J. Appl. Phys.* **1967**, *38*, 1289.

(17) (a) del Monte, F.; Morales, M. P.; Levy, D.; Fernandez, A.; Ocana, M.; Roig, A.; Molins, E.; O'Grady, K.; Serna, C. J. *Langmuir* **1997**, *13*, 3627. (b) Cotton, F. A.; Wilkinson, G. *Advanced Inorganic Chemistry*; Interscience Publishers: New York, 1962; p. 709.

(18) Cao, X.; Prozorov, R.; Koltypin, Y.; Kataby, G.; Felner, I.; Gedanken, A. *J. Mater. Res.* **1997**, *12*, 402.

(19) Cornell, R. M.; Schwertmann, U. *The Iron Oxides? Structure, Properties, Reactions, Occurrence and Uses*; VCH: Weinheim, 1996.

(20) Feitknecht, W.; Mannweiler, U. *Helv. Chim. Acta* **1967**, *50*, 570.

(21) Sidhu, P. S. *Clays Clay Miner.* **1988**, *36*, 31.

(22) David, R. L., Ed. CRC Handbook of Chemistry and Physics, 78th ed.; CRC Press: Boca Raton, 1997−1998; pp 12−14.

(23) Ramselaar, W. L. T. M.; Craje, M. W. J.; Hadders, R. H.; Gerkama, E.; deBeer, V. J. H. *Appl. Catal.* **1990**, *65*, 69.

(24) Hoffmann, D. P.; Houalla, M.; Proctor, A.; Fay, M. J.; Hercules, D. M. *Appl. Spctrosc.* **1992**, *46*, 208.

(25) Carbucicchio, M. *J. Chem. Phys.* **1979**, *70*, 784.

(26) Vaishnava, P. P.; Montano, P. A.; Tischer, R. E.; Pollack, S. S. *J. Catal.* **1992**, *77*, 29.

(27) Vuurman, M. A.; Wachs, I. E. *J. Molecular. Catal.* **1992**, *77*, 29.

(28) Willshee, J. C.; White, J. *Trans. Br. Ceram. Soc.* **1968**, *67*, 271.

(29) White, J. *Phase Diagrams: Materials Science and Technology*; Alper, A. M., Ed.; Academic Press: New York, 1970; Vol. 2, p 21.

(30) Lee, H. Y.; Paek, Y. K.; Lee, B. K.; Kang, S. J. L. *J. Am. Ceram. Soc.* **1995**, *78*, 2149.

(31) Nakamoto, K. *Infrared Spectra of Inorganic and Coordination Compounds*; John Wiley & Sons: New York, 1963; p 180.

(32) Morteera, C.; Emanuel, C.; Cerrato, G.; Magnacca, G. *J. Chem. Soc., Faraday Trans.* **1992**, *88*, 339.

(33) Mizushima, Y.; Hori, M. *J. Non-Crystal Solids* **1994**, *167*, 1.

(34) Kosmas, C. S.; Franzmeier, D. P.; Schulze, D. G. *Clays Clay Miner.* **1986**, *34*, 625.

(35) Vuurman. M. A.; Stufkens, D. J.; Oskam, A.; Deo, G.; Wachs, I. E. *Chem. Soc., Faraday Trans.* **1996**, *92*, 3259.

(36) Segawa. K.; Hall, W. K. *J. Catal.* **1982**, *76*, 133.

(37) Knozinger, H.; Ratnasamy, P. *Catal. Rev.−Sci. Eng.* **1978**, *17*, 31.

(38) (a) Peri, J. B. *J. Phys. Chem.* **1960**, *64*, 1526. (b) Peri, J. B. *J. Phys. Chem.* **1965**, *69*, 220.

(39) Datta, A. *J. Phys. Chem.* **1989**, *93*, 7053.

(40) Dai, Q.; Robinson, G. N.; Freedman, A. *J. Phys. Chem. B* **1997**, *101*, 4940.